2001 The Visualization Society of Japan and Ohmsha, Ltd.
Journal of Visualization, Vol. 3, No. 4 (2001) 357-367

McCutcheon, G.*[1], McColgan, A. H.*[1], Percario, S.*[2], Hurst, D.*[3] and Grant, I.*[1]

*1 Fluid Loading and Instrumentation Centre, Heriot-Watt University, Edinburgh, Scotland, EH10 5PJ, UK.
*2 Mechanics and Aeronautics Dept., University of Roma "La Sapienza," Via Eudossiana 18, 00184 - Rome, Italy.
*3 Department of Aerospace Engineering, University of Glasgow, Glasgow, Scotland, G12 8QQ, UK.

Received 22 August 2000.
Revised 17 January 2001.

***Abstract*:** The common optical configuration for two-component, particle tracking studies places the light sheet such that the mean velocity vector is coplanar with the illuminated area. In other, innovative studies, it has been found advantageous to place the sheet normal to the mean flow. Using this geometry it is necessary to apply a correction to the perceived, in-plane particle displacements to allow for the systematic error due to through-sheet motion. This correction has been made in the past by assuming a constant, through-sheet velocity, necessitated by the limited two-component measurement regime. This paper describes the errors in obtaining in-plane velocity components when assuming, constant, through-sheet motion. An illustration is presented where the viewing corrections were applied to images obtained in the study of the wake of a model road vehicle using PTV in the Particle Tracking Velocimetry (PTV) mode. Assuming a constant through-sheet velocity, it was shown that there were potentially, significant errors in the measured velocity. This was confirmed by measuring the freestream velocity at a matrix of points on the sheet then comparing the calculated in plane-motion using this variable in-plane velocity for correction. The differences in the velocity, drag and lift distributions and total induced drag and total lift using this approach were calculated and are reported in this paper.

***Keywords*:** particle tracking velocimetry, particle image velocimetry, through-sheet velocity correction, wake survey, aerodynamics, road vehicles, induced drag.

***Nomenclature*:**

b	distance moved in freestream direction
c_l	sectional lift coefficient
c_{dj}	sectional induced drag coefficient
d	object distance
D_i	total induced drag
h	model height (mm)
i	image distance
j, k	uniform grid parameters
L'	lift per unit span
N	number of vectors
t	time delay between two pulses
U_M	measured freestream velocity
U_∞	constant freestream velocity
u, v, w	velocity components in x, y, z directions
W	indicates an integral confined to the wake
X	distance from the datum line on the model
x, y, z	rectangular Cartesian coordinates
z_c	confidence coefficient

Greek symbols

$\boldsymbol{e_m}$	fractional error
$\boldsymbol{s}$	standard deviation
$\boldsymbol{m}$	true mean velocity
$\boldsymbol{r}$	density of air
$\boldsymbol{r}_\infty$	freestream density of air
	transverse component of vorticity
$\boldsymbol{G}$	circulation
$\boldsymbol{y}$	transverse component of stream function

In two-component, Particle Tracking Velocimetry (PTV) studies, where the light sheet is not co-planar with the mean flow, correction procedures have been developed (Grant et al., 1994) to eliminate the apparent in-plane motion due to through-sheet flow. This approach has allowed ambitious, large scale, experimental programmes to be successfully completed (Grant et al., 1999).

Recently, PTV has been applied to road vehicle wake diagnostics and has provided valuable insights into this important and challenging environment (McCutcheon et al., 2000 ; Wang et al., 1996). Little previous work has been reported in this topic so the present investigation has proven of great interest to the industry.

This paper describes the two-stage experiment which obtained three-component, two dimensional data in the wake of a road vehicle model. A light sheet was aligned normal to the mean flow in order to obtain the wake characteristics. The results showed that the instantaneous flow structure in the cross-plane was dramatically different from the measurement obtained by time-averaged techniques.

In correcting for the parallax effect around the edges of the PTV pictures, the local streamwise velocity has, in the past, been assumed to be the same as the freestream velocity. In the present study it was shown that this leads to significant errors and that measured through sheet values are required if a reliable correction procedure is to be implemented.

The experiments were conducted in the closed-return, low-turbulence, wind-tunnel in the Fluid Loading and Instrumentation Centre, Department of Civil and Offshore Engineering, Heriot-Watt University. The tunnel was used in a free-jet configuration to enable easy optical access and to minimize blockage effects. The open working section was 2.3m long and the octagonal outlet measured 1.2m between the opposite flat surfaces with each surface being 0.51m long. A maximum wind-speed of 20m.s^{-1} was used, which gave a Reynolds number of 6.0×10^5, based on model length.

The model used was a representation of a hatchback car and is shown in Fig. 1. The wind-tunnel did not have a moving ground facility and a stationary ground board was positioned at a distance of 21% of model height below the model. Although this arrangement does not fully simulate a car on the road, Hackett et al. (1987) showed that the induced drag acting on a bluff model vehicle, in a rolling road configuration, compared well with that obtained with the model over a stationary ground plane. In the present instance, as the simulated stationary road had a finite thickness, the ground board was fitted with an aerodynamic leading edge and a variable tail flap to provide steady test conditions and allow the pressures above and below the road to be adjusted.

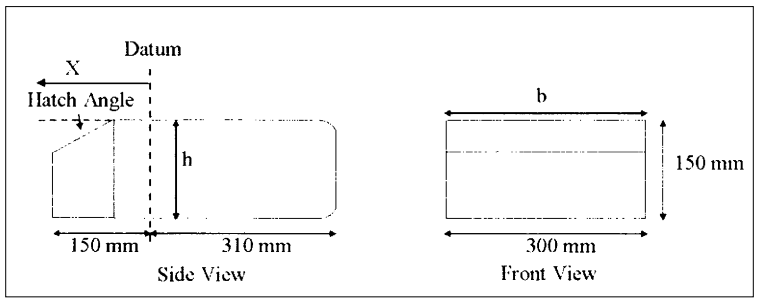

Fig. 1. Model dimensions.

The model had no added features such as wheels, side mirrors, aerials, engine-cooling ducts etc. The model had no added peripheral features, such as wheels and side mirrors, so that the typical flow features observed would have wide application and interest. A more complete description of the model test programme and results can be found in McCutcheon et al. (2000) and McCutcheon et al. (2001).

Strobe illumination for the PTV measurements was provided by two DCR-11, pulsed Nd:YAG lasers. By employing a system of lenses and mirrors, a vertical light sheet of suitable thickness was used at a number of test positions downstream of the model. The seeding particles used were synthetic polycrystalline particles with an

average diameter of 8***m***m providing sufficient scattering of light. These seeding particles were injected into the flow downstream of the model, by means of a seeding rake attached to a pressurised reservoir of particles. With suitable combinations of time delay, laser sheet thickness and camera settings, good spatial resolution was obtained in the film and electronic photographic images.

For the wake survey, the light sheet was perpendicular to the airflow with the camera situated downstream of the model and facing perpendicular to the light sheet and into the airflow. Images were obtained at four positions downstream of the model. These positions were non-dimensionalised using the model height (150mm). The measurement planes were situated at distances of X/h = 2.5, 3.3, 4.17 and 5.0 from the datum mark on the model (refer to the white marks on the ground plane of Fig. 2). The angle of the hatchback of the vehicle was 25° for all 4 wake survey positions. In further tests at position X/h = 4.17, the hatchback angle was varied with wake surveys at angles of 25°, 30° and 35° being investigated.

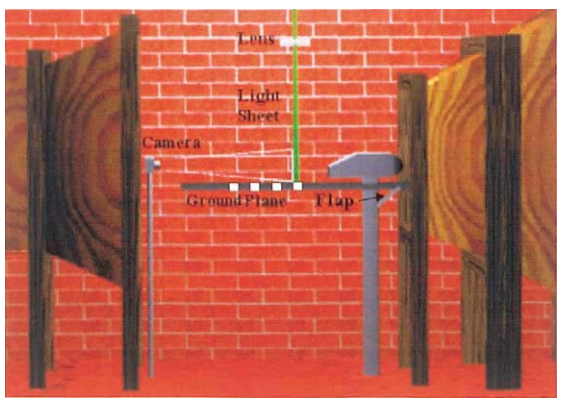

Fig. 2. Wind-tunnel set up.

The PTV images, of the light sheet normal to the mean flow, were recorded, using a Nikon F302 SLR 35mm, SLR camera with Nikon 55mm and 50mm macro lenses. The images were recorded on Kodak TMax 400 film and digitised using a Nikon Coolscan to obtain a resolution of 0.0156 mm/pixel. The general methodology in particle tracking has three principle features. These are the removal of noise by a suitable filtering method, the location of the particle image centroid and the matching of the particle images. Based on the work by Grant and Lui (1989), the procedures were carried out with an improved edge detection algorithm based on Laplacian operation to detect the image boundaries.

The measurements of stream-wise velocity were obtained by orientating the light sheet so that it was co-planar with freestream velocity and the vertical. PTV images were then obtained using a Pulnix CCD camera fitted with a Nikon 55mm macro lens. The light sheet was consecutively placed in a grid of positions at 50mm spacing in the y direction and 10mm spacing in the z direction. To obtain useful PTV measurements, it was necessary to average many images with identical spatial windows at random, or independent instances in time. Since these measurements were not simultaneously obtained with the through-sheet measurements, consideration has been given here to the confidence limits or accuracy of the flow parameters obtained as a function of the number of vectors in order to evaluate the significance of the averaging procedure.

The principle consideration in sampling theory is the number of vectors that must be obtained to report the flow parameters with a given accuracy (Grant and Owens, 1989). Statistical sampling theory can then be used to obtain accuracy estimates. The true mean velocity $\boldsymbol{m}$ and the standard deviation $\boldsymbol{s}$ were obtained where the fractional error $\boldsymbol{e}_m$, in estimating the mean, was obtained from

$$\boldsymbol{e}_m = \frac{z_c \boldsymbol{s}}{\boldsymbol{m}\sqrt{N}} \tag{1}$$

z_c is the confidence coefficient, or critical value, and can be obtained from normal curve tables. This analysis used a 95% confidence level with the acceptation of 5% or less for the fractional error. This requirement only excluded small areas of the wake where the flow was very turbulent and unsteady where the error reached 5%. This

confirmed that the time averaged stream-wise velocity had a small variance and could acceptably be used to make an improved viewing angle correction to the transverse wake images.

The correction for the viewing angle applied to PTV data has previously been reported in detail (Grant et al., 1994). The seeding particles were assumed to pass through the light sheet (x direction) at the freestream velocity while also, independently, moving in the y and z directions (in-illumination-plane co-ordinates). If the distance moved in the freestream direction, normal to the light sheet between exposures was b, then the transformations for the two image points (y_1, z_1, $b/2$) and (y_2, z_2, $-b/2$) of each particle are different (Fig. 3). This value of b has been assumed constant in previous work. Equation (2) shows its relationship to the measured freestream velocity U_M, and time delay between the two illumination pulses of the laser, t. In the present case, the measured freestream velocity was used to obtain the true displacement of the particles. The points (y_{01}, z_{01}) and (y_{02}, z_{02}) are the corresponding images on the film.

$$b = U_M t \tag{2}$$

$$y_1 = \frac{d + b/2}{i} y_{01} \qquad z_1 = \frac{d + b/2}{i} z_{01}$$

$$y_2 = \frac{d - b/2}{i} y_{02} \qquad z_2 = \frac{d - b/2}{i} z_{02} \tag{3}$$

These transformations relate the measured displacement in the film plane to the actual displacement in the plane of the light sheet.

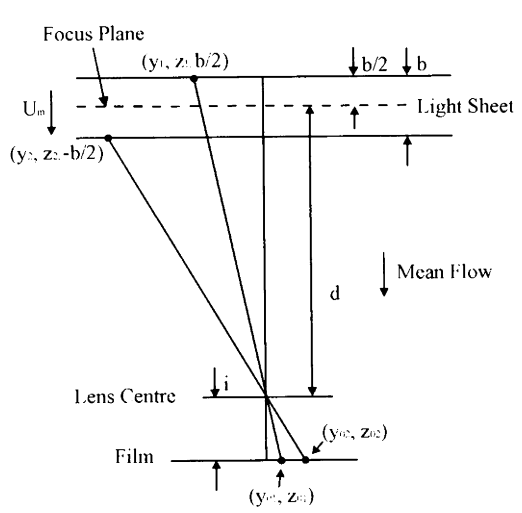

Fig. 3. Geometry for through-sheet motion.

Prior to testing, in each case, a target consisting of a precision grid was placed in the light sheet and photographed in order to calibrate magnification of the system.

The geometry of the present wake study was such that the through sheet motion of the mean flow provided the best opportunity for observing the development and dissipation of the shed vorticity from the model vehicle. The mean, freestream flow was always effectively parallel to the main wind-tunnel axis making the principal component normal to the light sheet. Measurements were made with the camera axis parallel to the freestream flow. With this set up, a 'starburst' effect was observed. The optical arrangement meant that in a double exposure, as a particle translated through the light sheet, the magnification was different at the initial (y_1, z_1) and final particle positions (y_2, z_2) (See Eq. (3)). There is a systematic increase in the first particle position, after correction, with the distance from the optical axis. There is a systematic decrease in the second particle position, after correction, with distance from the optical axis. This means that velocity vectors whose directions were inwards before correction, are stretched. Vectors whose directions were outwards before correction, are compressed.

The correction procedure first identified the position of the optical axis of the camera. The starting points and end points of each vector were identified and independently transformed with its respective measured through-sheet velocity U_M. Figure 4 clearly shows the 'starburst' effect of the raw uncorrected vectors in the wake of the model vehicle at survey location X/h = 2.5. Figure 5 shows the resulting velocity field, after correction, using the measured through sheet velocity at each wake position. It clearly demonstrates the instantaneous wake was dominated by two contra-rotating primary trailing vortices, which interacted with the ground plane, and produced

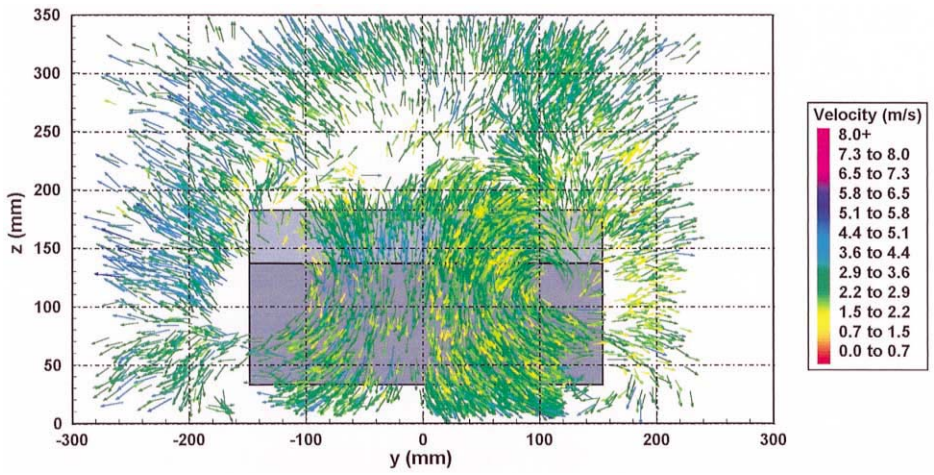

Fig. 4. Velocity field before correction.

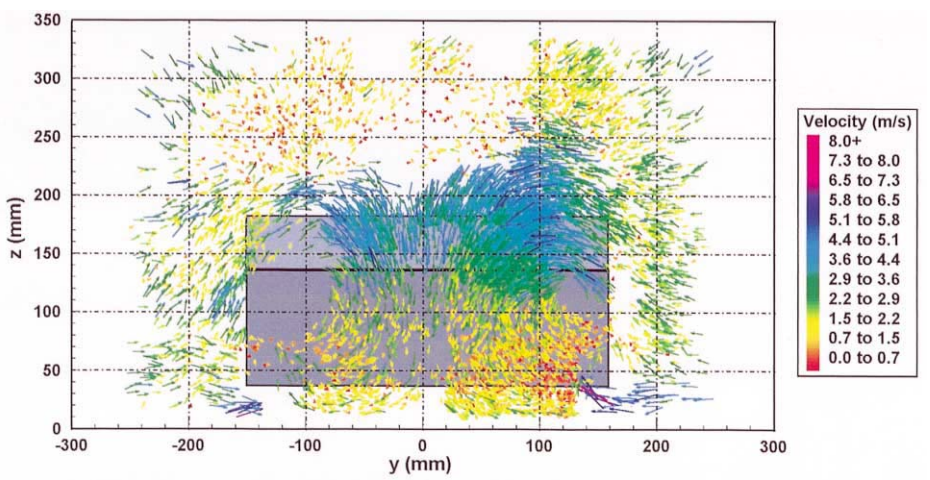

Fig. 5. Velocity field after correction.

two smaller, secondary vortices rotating in the opposite direction to their respective primary vortices. These secondary vortices are a result of the ground skin-friction effects.

The error U_E in the y and z components of velocity is the difference between the constant freestream velocity U_∞ and the measured through-sheet velocity U_M such that

$$U_E = U_\infty - U_M \tag{4}$$

Figure 6 shows the errors for wake location X/h = 2.5 with interpolated corrected vectors added to indicate the flow direction. It was evident that there were significant differences at the centre of the vortices. This meant, that assuming a constant through-sheet velocity, there can be a maximum difference of nearly 2m.s^{-1} error in those areas. The actual velocity of the vectors, shown in Fig. 5, had a maximum of 5m.s^{-1}, which represented a possible error of 40%. There is also a significant difference in the lower middle region of the wake, seen as the areas of dark blue. The value of velocity here had a maximum difference of 1.5m.s^{-1} which meant a possible error of 50%

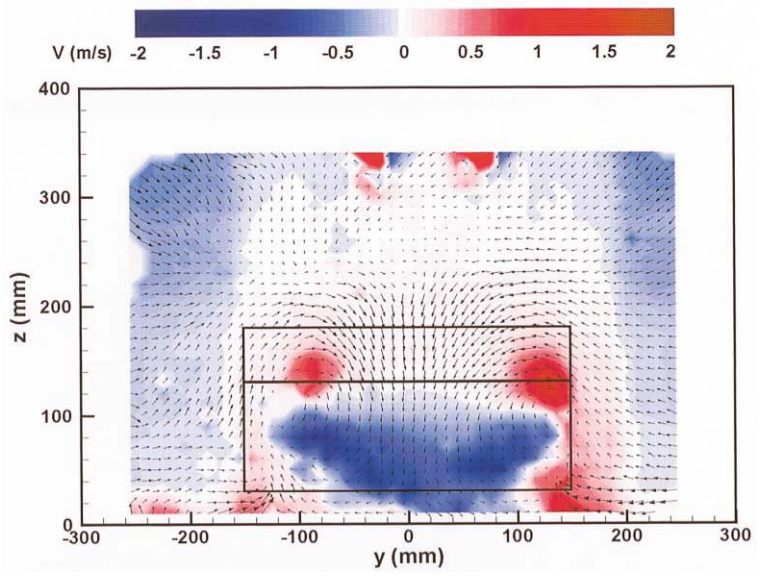

Fig. 6. Error in velocity.

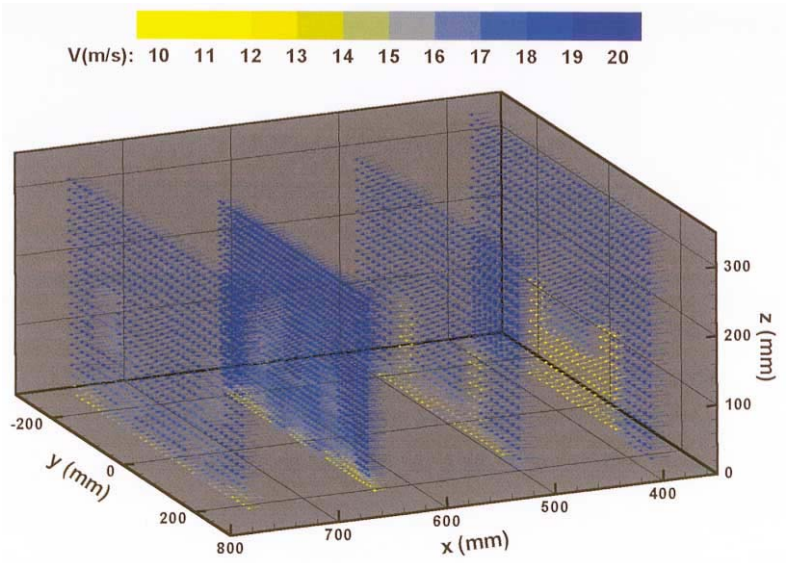

Fig. 7. Two stage 3-D velocity profile.

since the corrected image, Fig. 5, had a maximum value of velocity of about 3 m.s^{-1} in that area.

Figure 7 demonstrates the variation in measured freestream velocities at the four wake survey positions. This was obtained in two stages. The first stage was to obtain the v and w velocities component is the y, z plane (cross-flow wake-survey planes). The second stage was to obtain the x component of velocity U_M for each of the four survey positions at various heights as to obtain a profile of the entire wake (explained in Sections 3 and 4). Although this three-dimensional analysis was done in two stages, it still demonstrated the importance of obtaining the x-component of the velocity vectors. The three-dimensional plot clearly shows that near the model vehicle, 375mm (X/h = 2.5), the through-sheet velocity is about 10-12m.s^{-1}. As the vortices dissipate downstream, the x component of the vectors approach the freestream velocity of 20m.s^{-1}. This phenomenon has not been discussed in previous studies in this area. The present study has demonstrated that assuming the through-sheet velocity to be constant, when applying the correction transformations, is inappropriate and prone to errors. In the following section a method for calculating induced drag from the PTV measurements is described and the potential errors in this calculation if uniform through-sheet motions is assumed, rather than measured.

6.1 Induced Drag Measurement from PTV Wake Data

The most common technique used to measure lift and drag on bodies is to use a force balance in a wind tunnel. This method is susceptible to errors when evaluating the drag, due it being an order of magnitude less than the lift force. The model support also contributes to this error. An alternative method is to use a wake traverse approach which involves obtaining pressure and velocity readings in the wake of the model. Assuming an incompressible flow, and applying the momentum integral method to a control volume, Maskell (1973) developed Betz's theorem, resulting in an expression for the total drag on a lifting body. Maskell found that the induced drag on a lifting body could be expressed by

$$D_i = \frac{1}{2}\boldsymbol{r}\iint_W \boldsymbol{y}\ \ dS \tag{5}$$

Cummings et al. (1996) then related this equation to calculated local values of circulation and stream function, resulting in the induced drag being obtained for each column of data on a regular interpolated grid, Eq. (6).

$$D_i = \frac{1}{2}\boldsymbol{r}_\infty \sum_{j,k}\frac{1}{4}(\boldsymbol{y}_{j,k} + \boldsymbol{y}_{j+1,k} + \boldsymbol{y}_{j,k+1} + \boldsymbol{y}_{j+1,k+1})\boldsymbol{G}_{j+1/2,k+1/2} \tag{6}$$

The local circulation, $\boldsymbol{G}_{j+1/2,k+1/2}$, is related to the local vorticity, $_{j+1/2,k+1/2}$, as follows

$$_{j+1/2,k+1/2} = \frac{\boldsymbol{G}_{j+1/2,k+1/2}}{y\ \ z} \tag{7}$$

The calculation of the lift distribution along a lifting body was then obtained by a wake integration of vorticity. Using the Kutta-Joukowski theorem, Eq. (8), the lift per unit span at a y position along the lifting line can be obtained.

$$L'(y) = \rho_\infty U_\infty \boldsymbol{G}(y) \tag{8}$$

Calculating a wake summation of shed circulation or wake area integration of shed vorticity, the bound circulation values at points of interest along the lifting body can be found. Equation (9) represents the discretized representation for integrating the shed stream-wise vorticity over the uniform grid.

$$\boldsymbol{G} = \sum_{j,k}\ _{j+1/2,k+1/2}\ \ y\ \ z \tag{9}$$

6.2 Errors in Wake Survey at X/h = 2.5

Figures 8 and 9 show the induced drag and lift distributions at wake survey location X/h = 2.5, respectively. The error bars due to the time-averaged technique used have been added to both the measured induced drag and lift

curves. From the induced drag curves, it is clear that assuming a constant freestream velocity, the calculated induced drag is systematically reduced over the span of the vehicle. This effect is an order of magnitude larger than the errors due to the time averaging approach. The lift curve behaved in the same manner in that there are more negative regions of lift for the constant freestream velocity case causing an over all reduction in the total lift value. Again, this effect is an order of magnitude greater than the error bounds in the time-averaged measured values.

6.3 Downstream Errors in the Wake

Figure 10 shows the total values of induced drag for the four downstream positions. Both the measured and freestream plots behave in the same manner in that the induced drag decreases downstream of the model. By assuming a constant through sheet velocity, the resulting values of induced drag can lead to a 23% error in some cases (see Fig. 11 for percentage values for the four survey locations).

Bearman et al. (1983) showed the induced drag for a hatch back car of 25° at wake survey location X/h = 4.17, to account for 23% of the total drag of the vehicle. This would mean an error of 3.5% of the total drag would

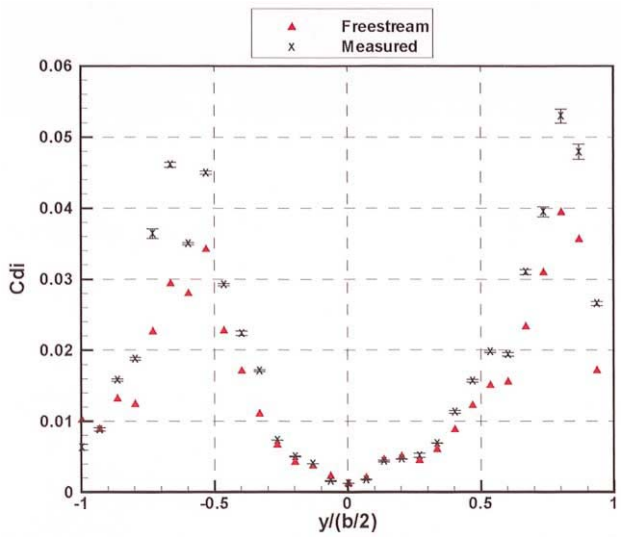

Fig. 8. Drag distribution at X/h = 2.5.

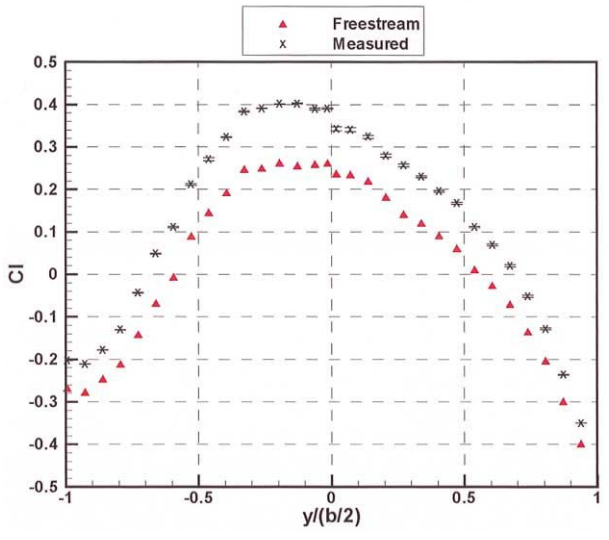

Fig. 9. Lift distribution at X/h = 2.5.

occur since the error between constant and measured freestream velocity is nearly 15%. Ahmed (1981) showed this induced drag to constitute 28% of the total drag for a hatch back of 22.5° at survey location X/h = 2.08. This is similar to the current survey location of X/h = 2.5 with hatch angle 25°, allowing a comparison. The error in drag at this position is 16%, which means an error of 4.48% on the total drag. These two examples demonstrate the importance that errors in the induced drag can have on the total drag.

Figure. 12 demonstrates that assuming a constant freestream velocity leads to very significant errors for the total lift values. The percentage error bar chart, Fig. 13, clearly shows very high percentage errors with a maximum of 332%.

This paper has discussed the errors in assuming a constant through-sheet velocity when applied to the correction for the viewing angle. Although the through-sheet velocity was time averaged, the velocities, obtained instantaneously, did not differ more than 5% from the averaged values and thus allowed as systematic study of the likely errors in wake measurements previously obtained using an assumed constant, through-sheet velocity. Since velocity is used directly in the calculation of induced drag and lift, errors in the calculated values of these parameters were also examined. This was repeated at positions over the span of the model vehicle wake at various downstream positions.

The total induced drag values for both the measured, and freestream, through-sheet velocity showed the

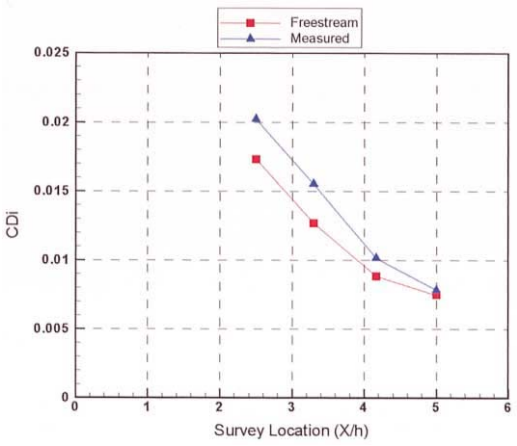

Fig. 10. Total induced drag.

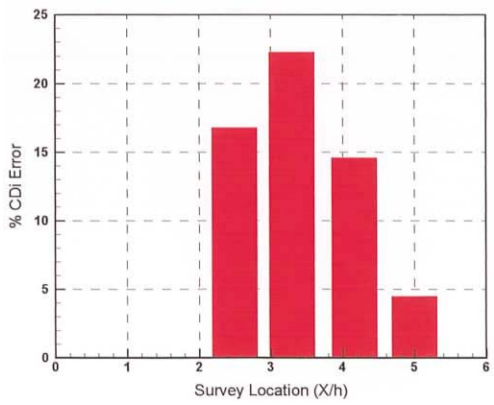

Fig. 11. % Error of total induced drag.

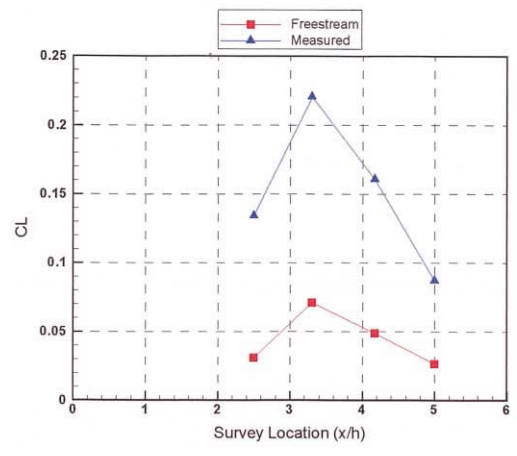

Fig. 12. Total lift.

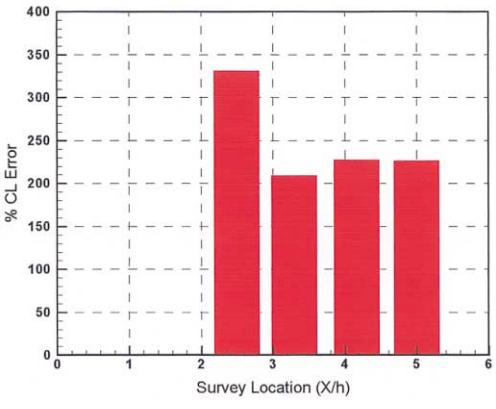

Fig. 13. % Error in Total lift.

same trend but with significant differences in magnitude. The errors in total lift were substantial. The total values of induced drag showed an error of 23% in some cases. The induced drag has been shown to represent 23% of the total drag of a hatch back vehicle at a survey location X/h = 4.17 and 28% at X/h = 2.5. This would result in an error of about 3.5% and 4.48% for the total drag, respectively.

With these wake survey techniques, detailed flow characteristics were obtained. Ideally, instantaneous three-component data should be used in measuring and calculating wake flows and their derived quantities. However, it has been shown that time averaged, stream-wise measured velocities provide an accurate and significant improvement in estimating induced drag and lift from PTV wake measurements. Given the substantial effect on the lift force, constant through-sheet velocity should not be assumed when correcting in-sheet motion for viewing angle.

Acknowledgments

The authors acknowledge the suggestion from Dr. N. Taylor (formerly DERA, Farnborough) to consider the Betz-Maskell work in relation to obtaining induced drag from to PTV measurements.

References

Ahmed, S. R., Wake Structure of Typical Automobile Shapes, Transactions of the ASME, Vol. 103, (1981).

Bearman, P.W., Davis, J. P. and Harvey, J. K., Measurements of the Structure of Road Vehicles Wakes, Int. Journal of Vehicle Design, Special Publication SP3, (1983).

Cummings, R. M., Giles, M. B. and Shrinivas, G. N., Analysis of the Elements of Drag in Three-dimensional Viscous and Inviscid Flows, AIAA 96, 2482, (1996).

Grant, I. and Lui, A., Method for the Efficient Incoherent Analysis of Particle Image Velocimetry Images, Applied Optics, 28 (1989), 1745-1748.

Grant, I. and Owens, E., Confidence Interval Estimates in PTV Measurements of Turbulent Flows, Applied Optics, 29 (1989), 1400-1402.

Grant, I., Pan, X., Wang, X and Stewart, N., Correction for Viewing Angle Applied to PTV Data Obtained in Aerodynamic Blade Vortex Interaction Studies, Experiments in Fluids, 18 (1994), 95-99.

Grant, I., Mo, M., Pan, P., Parkin, P., Powell, J., and Hurst, D., A PIV and LSV Study of the Wake of an Aircraft Model, Journal of Flow Visualization, 2, 1 (1999), pp. 85-92.

Hacket, J.E., Baker, J.B., Williams, J. E. and Wallis, S. B., On the Influence of Ground Movement and Wheel Rotation in Tests on Modern Car Shapes, Society of Automotive Engineers, 870245, (1987).

Maskell, E.C., Progress towards a Method for the Measurement of the Components of the Drag of a Wing of Finite Span, Technical Report 72232, Royal Aircraft Establishment, (1973).

McCutcheon, G., McColgan, A. H., Hurst, D. and Grant, I., Measurement of Aerodynamic Forces in the Wake of a Road Vehicle Using Wake Integration and PIV Techniques, Proc. 9th Int. Symposium on Flow Visualization (Heriot-Watt University, Edinburgh), (August 22-252000), paper 206, 206.1-206.11, (ISBN 09533991 1 7).

McCutcheon, G., McColgan, A.H., Hurst, D. and Grant, I., Wake Studies of a Model Passenger Car using PIV, to be presented at the 3rd Pacific Symposium on Flow Visualization and Image Processing, March 18-21 (2001).

Wang, Q., Bearman, P.W. and Harvey, J.K., A Study of the Instantaneous Flow Structure Behind a Car by Particle Image Velocimetery, Optical Methods and Data Processing in Heat and Fluid Flow, IMechE Conference Transaction, (1996-3), 179-188.

Author Profile

Gordon McCutcheon: He is a graduate of Glasgow University, obtaining a Masters in Aeronautical Engineering in 1998. He has worked with Military Aircraft at British Aerospace, UK and researched the development of a Mexican designed satellite for Supaero University, Toulouse, France. He will complete his PhD from Heriot-Watt University in September 2001. Research activities include a PIV study of vehicle and wing aerodynamics. Present research includes the study of aerodynamic loading using wake integration techniques and developing a three dimensional PIV system.

Andy McColgan: He is currently a Ph.D student and his research focuses on typical car and racecar aerodynamics. He obtained his BEng in Aeronautical Engineering from the University of Glasgow in 1998. His work in the past has been on a computational study of low-speed aerofoils and high-lift configuration wings. His present work includes an experimental study of Gurney Flap aerodynamics.

Stephano Percario: He will obtain his degree in Aeronautical Engineering from the University of Roma "La Sapienza". Arriving at Heriot-Watt as part of the ERASMUS student exchange program, he soon developed valuable skills in the field of PIV and contributed immensely to the current research activities.

Dave Hurst: He was a senior Lecturer in the Department of Aerospace Engineering at Glasgow University. A previous research lecturer at Southampton University, he has held numerous awards including the Spitfire Mitchell Research Scholarship and visiting scholar at VKI. He has published widely in the areas of bluff body dynamics, lifting surfaces, e.g. aircraft propellers and race car aerodynamics. He has currently taken a position with Jaguar Formula One Racing, UK.

Ian Grant: He obtained a degree in Physics from the University of Edinburgh in 1969 and a PhD in 1972. He holds a personal chair at Heriot-Watt University. His main area of work is the development and application of optical, image processing, PIV and neural techniques in engineering. He has published more than 140 papers and was Editor of the SPIE Milestone Volume on PIV. He is a founding editor of the e-journal 'Optical Diagnostics in Engineering,' was joint editor responsible for electronic proceedings at the 8th International Symposium on Flow Visualization (Sorrento, 1998). He was Chairman and joint editor of the 9th Symposium (Edinburgh, 2000).